

## Associative Ionization with Cold Rydberg Lithium Atoms

M. W. McGeoch, R. E. Schlier, and G. K. Chawla

*Avco Research Laboratory, 2385 Revere Beach Parkway, Everett, Massachusetts 02149*

(Received 15 April 1988)

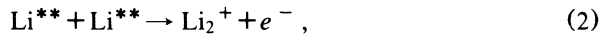
Rydberg-atom-Rydberg-atom associative ionization was measured in lithium at 85 K for principal quantum numbers 3, 5, and 9. The very high rate constants, up to  $10^{-7} \text{ cm}^3 \text{ s}^{-1}$ , were modeled by considering the binding between the ion and the Rydberg atom which result from an initial ionizing collision. A search for evidence of ion pair production yielded an upper bound on its rate constant of  $3 \times 10^{-10} \text{ cm}^3 \text{ s}^{-1}$  for  $n=9$ . Lithium negative ions observed in the experiment were produced by attachment.

PACS numbers: 34.50.Fa, 34.60.+z

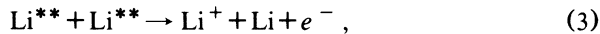
Following a recent report<sup>1</sup> of a very high rate of ion pair production in Rydberg-Rydberg sodium collisions we looked for evidence of the analogous process



in lithium. We observed an extremely high rate constant ( $\sim 10^{-7} \text{ cm}^3 \text{ s}^{-1}$ ) for associative ionization



but no evidence of process (1) even in the conditions of high Rydberg density which were optimum for process (2). Process (2) is observed to compete on equal terms with collisional ionization



which, like (2), has an excess energy of several eV, but apparently should have a much greater density of final states. Our explanation invokes the long-range binding of  $\text{Li}_2^+$  (which is analogous to that for  $\text{H}_2^+$ ) and leaves most of the energy within the  $\text{Li}_2^+$  molecule in the form of electronic and nuclear excitation.

The present work involves pulsed laser optical excitation of Li atoms in a supersonic beam at densities up to  $1.3 \times 10^{13} \text{ cm}^{-3}$  and translational temperatures as low as

70 K.<sup>2</sup> The apparatus has been described previously.<sup>2</sup> The beam density was determined by the trapped decay lifetime of optically pumped  $\text{Li}(2p)$  states with use of Holstein's relationship<sup>3</sup> for the escape factor on a Doppler-broadened line. A similar method has been used by others.<sup>4</sup> The decay at two oven temperatures is given in Table I. Higher oven temperatures imply lower Doppler widths, greater densities, and increased resonant trapping in the beam. Because the  $\text{Li}(2p)$  population can remain high for longer than the  $\text{Li}^{**}$  radiative lifetimes ( $n=3$  to  $n=9$ ) the  $\text{Li}^{**} \rightarrow \text{Li}(2p)$  decay transitions can also be trapped, causing an observable lengthening of the Rydberg decay lifetimes at higher Li oven temperatures.

Optical excitation of Li is via  $\text{N}_2$ -laser-pumped dye lasers in oscillator-amplifier pairs. Each pair emits at 30 Hz tunable light pulses of duration 3 ns, energy  $10 \mu\text{J}$ , and bandwidth  $0.25 \text{ \AA}$ . The first excitation step is the  $\text{Li}(2s-2p)$  resonance transition at 671 nm. The second step is via a photon in the range 350–610 nm which accesses principal quantum numbers in the range 3 to 9, either in the  $s$  or  $d$  angular momentum state. The second-step laser intensity is varied through the use of neutral-density filters calibrated for the wavelength in question.

TABLE I. Comparison of Rydberg radiative lifetimes and  $\text{Li}_2^+$  formation times.

Optically pumped Li state	Radiative decay lifetime (ns)		$\text{Li}_2^+$ Formation time constant (ns) at different oven temperatures		
	To all lower states	Excluding decay to $2p$ state			
			795 °C	815 °C	835 °C
$8d$	293	735	...	$580 \pm 100$	...
$9d$	427	1050	$262 \pm 70$	$753 \pm 50$	$580 \pm 100$
$9s$	668	1210	...	$820 \pm 200$	...
$2p$	450 (772 °C)		...	...	...
	1740 (820 °C)		...	...	...
Beam temperature (K)			105	85	70
Li density ( $\text{cm}^{-3}$ )			$6.4 \times 10^{12}$	$9 \times 10^{12}$	$1.3 \times 10^{13}$

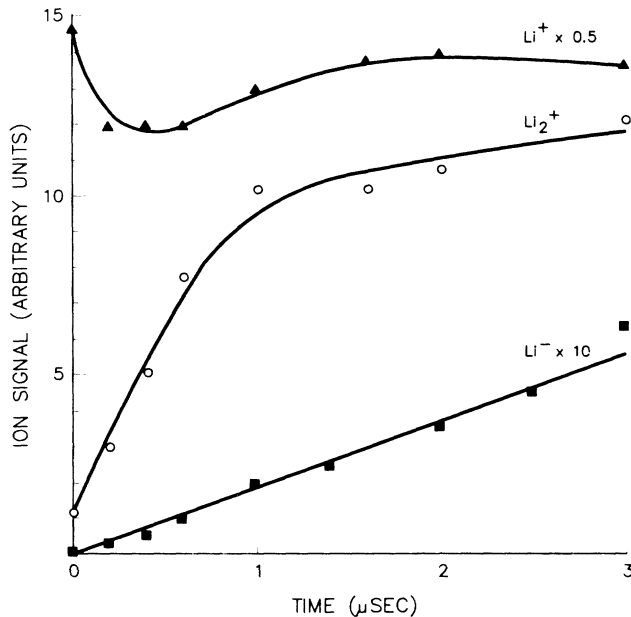


FIG. 1.  $\text{Li}^+$ ,  $\text{Li}_2^+$ , and  $\text{Li}^-$  signals as functions of time delay between optical excitation and ion extraction for  $8d$  excitation at optimum intensity for  $\text{Li}_2^+$ .

Ions produced either during optical excitation or in an interaction period of several  $\mu\text{s}$  thereafter are extracted by the application of a 400-ns, 2-kV pulse across two mesh electrodes situated 3.2 cm apart on either side of the beam. Depending on the polarity of this pulse either positive or negative ions can be sent down a 22-cm flight tube and detected (with approximately equal sensitivity<sup>5</sup>) by a Channeltron multiplier. In the flight tube there is a 200-G crossed magnetic field and a honeycomb transmission plate which stops the transmission of electrons. In the extraction direction opposite to the flight tube there is a Faraday cup for total-charge measurements of positive ions which are used to calibrate the Channeltron. The optically pumped volume is a cylinder of area  $0.031 \text{ cm}^2$  and length 0.86 cm. Ions are extracted in a direction perpendicular to the cylinder axis and species are resolved by time of flight.

The ions detected are exclusively  $\text{Li}^+$ ,  $\text{Li}_2^+$ , and  $\text{Li}^-$ . The time dependence of ion formation was studied by variation of the delay between the optical pump pulse and the extraction pulse. Time histories for excitation to  $nl=8d$  are shown in Fig. 1. Typically the  $\text{Li}_2^+$  signal develops over a period of  $<1 \mu\text{s}$  which is correlated below with the Rydberg decay lifetime. The level of the  $\text{Li}_2^+$  signal is, however, very sensitive to optical pump intensity on the  $2p \rightarrow nl$  transition. A typical laser-intensity dependence at fixed extractor delay of  $2 \mu\text{s}$  is shown in Fig. 2. Above an optimum pump intensity there is strong suppression of the  $\text{Li}_2^+$  signal. Below the optimum the  $\text{Li}_2^+$  signal scales as the 1.8 power of pump intensity indicating that the origin of the  $\text{Li}_2^+$  is mostly

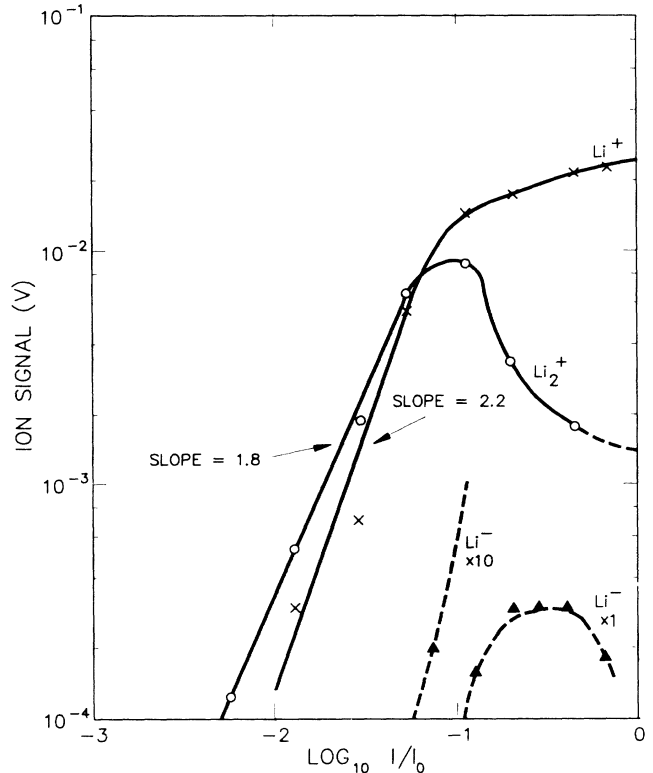


FIG. 2.  $\text{Li}^+$ ,  $\text{Li}_2^+$ , and  $\text{Li}^-$  signals as functions of laser intensity on the  $2p-9d$  transition at constant extraction time delay of  $2 \mu\text{s}$ . Intensity  $I$  is normalized to peak intensity  $I_0$ .

via Rydberg-Rydberg interaction (2). The suppression of associative ionization at high laser pump intensity has previously been noted in Sr (Ref. 6) and Na (Ref. 7), and attributed<sup>8</sup> to destruction of Rydberg states by an electron avalanche. Using the electron-Rydberg collisional rates of Devos, Boulmer, and Delpech<sup>9</sup> and our measured ion and electron density of  $\sim 3 \times 10^{10} \text{ cm}^{-3}$  near the optimum pump intensity for  $\text{Li}_2^+$  production, we note that the electron-avalanche explanation is consistent with the observed  $\text{Li}^{**}$  destruction at higher intensities.

The correlation of  $\text{Li}_2^+$  formation with  $\text{Li}^{**}$  radiative decay is further proof that  $\text{Li}_2^+$  forms via process (2), specifically from the  $\text{Li}^{**}$  state that is optically pumped. The formation rate of  $\text{Li}_2^+$  decays in an approximately exponential fashion (Fig. 1). Fitted-exponential formation time constants are compared in Table I with calculated  $nl$  radiative decay constants. Because  $\text{Li}_2^+$  formation is proportional to  $[\text{Li}^{**}]^2$ , its formation time constant should be equal to half of the  $\text{Li}^{**}$  radiative decay time constant. This appears to hold well for the data at  $795^\circ\text{C}$  but not so well at higher temperatures. It is expected that  $l$ -mixing collisions<sup>10</sup> will cause the formation of a reservoir of longer-lived  $nf$  states, so that the effective lifetime of an optically pumped  $nd$  state is increased, perhaps accounting for the discrepancy. Another

er complication is the expected contribution of superradiant emission.<sup>11</sup> In our conditions we calculate that the superradiant threshold is exceeded for  $n > 6$ , and that a fraction of  $n=9$  population will redistribute within  $10^{-8}$  s into  $n=8$ .

The  $\text{Li}^+$  signal varies as the 2.2 power of laser pump intensity on the  $2p \rightarrow nl$  transition, below the avalanche regime, indicating an origin via process (3). The  $\text{Li}^-$  signal for  $n=5$  and at a low intensity for  $n=9$  obeys a power law ranging between 1.5 and 2.0. However, the  $\text{Li}^-$  formation rate tends to increase with time out to at least  $3 \mu\text{s}$  (Fig. 1) ruling out ion pair production [process (1)] as the formation mechanism. Because the electron density has a second power dependence at low intensity, it is probable that  $\text{Li}^-$  formation in this regime is via dissociative attachment.<sup>2</sup>

Rate constants for process (2) with  $nl = 3d, 5d$ , and  $9d$  are shown in Fig. 3. These were derived from the following: the measured  $\text{Li}_2^+$  density; the calculated  $\text{Li}^{**}$  density ( $3 \times 10^{11} \rightarrow 8 \times 10^{11} \text{ cm}^{-3}$ ) derived from the Li density and the (in band) optical pump intensity; and the measured formation time of  $\text{Li}_2^+$ . They refer to  $l$  mixtures at principal quantum numbers 3, 5, and 9, the latter possibly  $n$  mixed to include 8 by superradiance. The error bars principally reflect uncertainty in the pumped volume. Analysis of our data for  $\text{Li}^-$  production allows us to place an upper bound of  $3 \times 10^{-10} \text{ cm}^3 \text{ s}^{-1}$  for ion pair production via process (1), with  $n=9$ .

A physical model for process (2) goes as follows: The first event in a Rydberg-Rydberg collision is the interaction of the orbital electrons leading to the ejection of one electron with a cross section given by Olson.<sup>12</sup> The remaining electron, if confined to one of the ionic cores, has to be demoted to an orbital  $N \leq n/\sqrt{2}$  if enough energy is released to ionize the other atom. The nascent  $\text{Li}_2^+$  complex [ $\text{Li}(N) \dots \text{Li}^+$ ] can be held together by the long-range ion-dipole interaction provided that the binding potential energy exceeds the kinetic energy of the two-particle system. Because the interaction energy of the ion and the Rydberg atom exceeds the  $l$  splitting of the atom, we may approximate the binding potential energy in  $\text{Li}_2^+$  by the asymptotic long-range potentials derived for  $\text{H}_2^+$  by Damburg and Propin.<sup>13</sup> The dominant long-range terms in the binding energy  $E_0$  are, in atomic units,

$$E_0 = \frac{3N\Delta}{2R^2} + \frac{N^2(N^2 - 6\Delta^2 - 1)}{2R^3} + \text{etc.}, \quad (4)$$

where  $R$  is the internuclear distance,  $\Delta = N_1 - N_2$  is the difference between parabolic quantum numbers subject to the constraints

$$0 \leq N_1 \leq N - |m| - 1, \quad 0 \leq N_2 \leq N - |m| - 1, \quad (5)$$

$$N = N_1 + N_2 + |m| + 1, \quad -(N-1) \leq m \leq N-1,$$

and  $m$  is the quantum number for angular momentum

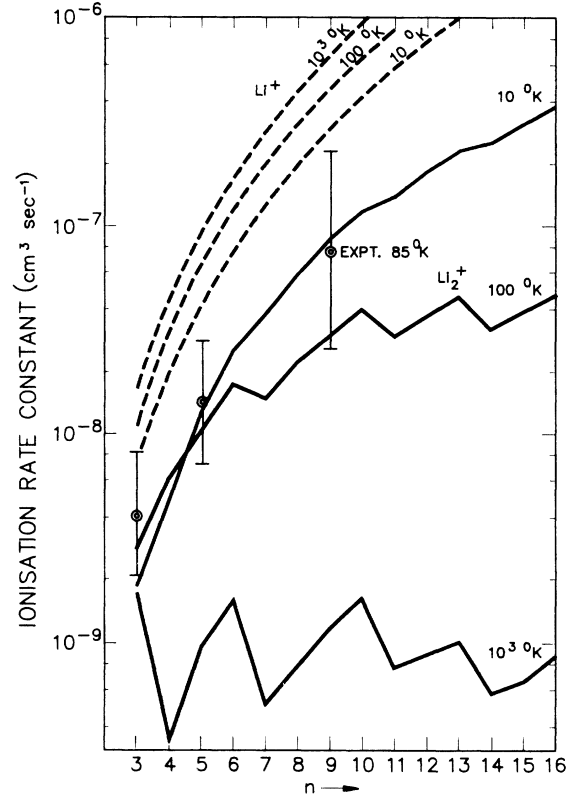


FIG. 3. Experimental rate constants for associative ionization at a beam temperature of 85 K. Rate constants for process (3) from Eq. (8) and the Olson calculation (Ref. 12) are shown as dashed curves. Rate constants for associative ionization from Eq. (9) are shown as full curves.

about the internuclear axis. The degeneracy of the  $\text{H}_2^+$  state characterized by  $(N, \Delta)$  is  $N - |\Delta|$ . Binding exists for  $E_0 < 0$ . For an ionizing collision which takes place at separation  $R$  with the Olson cross section, the  $\text{Li}_2^+$  complex is bound when the center-of-mass kinetic energy

$$\mu v^2/2 \leq -E_0(R). \quad (6)$$

In (6)  $\mu$  is the reduced mass,  $v$  is the asymptotic relative velocity of approach, and it is assumed that the neutral-neutral potential energy can be neglected relative to kinetic energy at separation  $R$ . The Olson cross section<sup>12</sup> may be parametrized in atomic units as

$$\sigma(n, v) = \pi R^2 = 0.703 v^{-0.65} n^{3.35} \quad (7)$$

in the region  $v/v_e \ll 1$ . We assume that all  $\text{Li}_2^+$  states satisfying  $N \leq n/\sqrt{2}$  are populated with equal probability. This gives weightings proportional to the degeneracy  $N^2$  (neglecting spin) and proportional to  $N - |\Delta|$  within a given  $N$  manifold. For lithium the lower bound of possible  $n$  states is 3, corresponding to  $N=2$ . The rate constant for the ionizing collision is

$$k(n) = \int_0^\infty \phi(v) \sigma(n, v) v dv, \quad (8)$$

where  $\phi(v) = 2p^2 v^3 \exp(-pv^2)$  is the distribution function of relative collision velocities<sup>14</sup> at temperature  $T$  with  $p = \mu/2kT$  ( $k$  is Boltzmann's constant). The rate constant for associative ionization is

$$k_{AI}(n) = \int_0^\infty \phi(v) \sigma(n, v) \mathcal{F}(n, v) v dv, \quad (9)$$

where  $\mathcal{F}(n, v)$  is the probability of binding after an ionizing collision, given by

$$\mathcal{F}(n, v) = \frac{1}{\sum N^2} \sum_N \sum_\Delta (N - |\Delta|) \delta(v), \quad (10)$$

where

$$\delta(v) = \begin{cases} 0, & v \geq v_{\max}, \\ 1, & v < v_{\max}. \end{cases}$$

Here,  $v_{\max}$  is the solution of (6) at equality. For any given set of  $(n, v)$  the interaction distance  $R$  is obtained from (7).

Calculated associative ionization rate constants are shown in Fig. 3 for different gas temperatures. We see that this simple model can explain the experimental data, which refer to 85 K. The curves show steps at points where  $N$  remains the same while  $n$  increases by unity, reflecting the constancy of the number of available states. We find that the calculated associative ionization rate constant is always less than half of the Olson rate constant for process (3) because  $\Delta$  ranges equally through positive and negative values in the leading term of (4), implying that at least half of the reactions enter repulsive  $\text{Li}_2^+$  states and dissociate to  $\text{Li}^+ + \text{Li}(N)$ . Experimentally we tend to observe more  $\text{Li}_2^+$  than  $\text{Li}^+$  at low laser intensity, but some uncertainty attaches to the relative efficiency of collection of the two species. In this model the  $\text{Li}^+$  ions tend to be formed at higher velocity and could be spreading into a larger volume before extraction.

Typical  $\text{Li}_2^+$  formation distances  $R$  are of the order of 100 a.u., so that what is formed is a fragile "planetary" molecule, which apparently survives for more than several microseconds in the beam environment, and also has a good probability of surviving extraction in an electric field of  $625 \text{ V cm}^{-1}$ . There are no  $\text{Li}_2^{2+}$  states available for autoionization below the  $\text{Li}^+ + \text{Li}^+$  asymptote.

When the  $l$  splitting exceeds the ion-Rydberg-atom interaction energy, as for example in other alkali metals in  $p$  states, the leading term is the ion-quadrupole or  $1/R^3$  term in (4). Evaluation of the associative ionization rate constant with only this term included leads to at least a factor of 300 lower rate constants (at 100 to  $10^3$  K). The model is inapplicable to  $\text{Na}(3p) + \text{Na}(3p)$ , including the 0.75-mK results of Gould *et al.*,<sup>15</sup> because in

this case insufficient energy exists for the initial atomic ionization. However, moderately high associative ionization rates are to be expected in alkali-metal Rydberg-Rydberg interactions. Some evidence for this in sodium has been reported by Burkhardt *et al.*<sup>7</sup>

In conclusion, we have observed a very high rate for associative ionization in low-temperature Rydberg-Rydberg lithium interactions. We have modeled the process by considering the long-range binding of  $\text{Li}_2^+$  states due to the ion-dipole force. We predict that the process is strongly temperature dependent, having its highest rate for the low-temperature conditions of our experiment. The relative absence of ion pair production is confirmed by the calculations of Michels and Montgomery<sup>16</sup> who do not find curve crossings to  $\text{Li}^+ + \text{Li}^-$  in the energy region that we have accessed.

It is a pleasure to acknowledge the experimental assistance of J. Gardner and support from the Air Force Office of Scientific Research via Contract No. F49620-87-C-0080.

<sup>1</sup>M. Ciocca, M. Allegrini, E. Arimondo, C. E. Burkhardt, W. P. Garver, and J. J. Leventhal, *Phys. Rev. Lett.* **56**, 704 (1986).

<sup>2</sup>M. W. McGeoch and R. E. Schlier, *Phys. Rev. A* **33**, 1708 (1986).

<sup>3</sup>T. Holstein, *Phys. Rev.* **83**, 1159 (1951).

<sup>4</sup>R. Bonanno, J. Boulmer, and J. Weiner, *Comments At. Mol. Phys.* **16**, 109 (1985).

<sup>5</sup>D. H. Crandall, J. A. Ray, and C. Cisneros, *Rev. Sci. Instrum.* **46**, 562 (1975).

<sup>6</sup>E. F. Worden, J. A. Paisner, and J. G. Conway, *Opt. Lett.* **3**, 156 (1978).

<sup>7</sup>C. E. Burkhardt, W. P. Garver, V. S. Kushawaha, and J. J. Leventhal, *Phys. Rev. A* **30**, 652 (1984).

<sup>8</sup>G. Vitrant, J. M. Raimond, M. Gross, and S. Haroche, *J. Phys. B* **15**, L49-55 (1982).

<sup>9</sup>F. Devos, J. Boulmer, and J.-F. Delpech, *J. Phys. (Paris)* **40**, 215 (1979).

<sup>10</sup>D. R. Herrick, *Mol. Phys.* **35**, 1211 (1978).

<sup>11</sup>F. Gounand, M. Hugon, P. R. Fournier, and J. Berlande, *J. Phys. B* **12**, 547 (1979).

<sup>12</sup>R. E. Olson, *Phys. Rev. Lett.* **43**, 126 (1979).

<sup>13</sup>R. J. Damburg and R. Kh. Propin, *J. Phys. B* **1**, 681 (1968).

<sup>14</sup>S. Chapman and T. G. Cowling, *The Mathematical Theory of Non-Uniform Gases* (Cambridge Univ. Press, Cambridge, 1953), Sec. 5.3.

<sup>15</sup>P. L. Gould, P. D. Lett, P. S. Julienne, W. D. Phillips, H. R. Thorsheim, and J. Weiner, *Phys. Rev. Lett.* **60**, 788 (1988).

<sup>16</sup>H. H. Michels and J. A. Montgomery, Jr., in *Production and Neutralization of Negative Ions and Beams—1986*, edited by J. G. Alessi, AIP Conference Proceedings No. 158 (American Institute of Physics, New York, 1987), p. 555.